Vol. 5 No. 2, Dec. 2025

FUAM Journal of Pure and Applied Science

Available online at
www.fuamjpas.org.ng

An official Publication of
College of Science
Joseph Sarwuan Tarka University,
Makurdi.

FUAM Journal of Pure and Applied Science
© College of Science, Joseph Sarwuan Tarka University, Makurdi
https://fuamjpas.org.ng/
Vol.5 No. 2 Dec. 2025

Radiation Dose Optimization in Computed Tomography Examinations: A comparative Analysis of Body and Head phantoms in some Radiological Units of Abuja Hospitals

J. T[1*]. Iortile, L[2]. Alumuku and A[3]. Shaanika
[1]Department of Radiology, Benue State University Teaching Hospital Makurdi, Nigeria
[2]Department of Pure and Applied Physics, Federal University Wukari, Wukari, Nigeria
[3]Ministry of Health and Social Services, Namibia
[*]Correspondence E-mail: iortileter@gmail.com

Received: 24/01/2025 **Accepted**: 01/04/2025 **Published online**: 02/04/2025

Abstract
The increasing use of Computed Tomography (CT) as a diagnostic modality in the country has raised a major concern of delivering high radiation dose and potential source of increased cancer risk. To address this concern, CT patient absorbed dose and Quality Control (QC) parameters during CT examinations at various radiological centres in Abuja were investigated using a Polymethyl Methacrylate (PTW chamber type 30009, Freiburg, Germany), 100 mm pencil ion chamber with PTW DIA DOS E integrated electrometer and a Victoreen CT probe, model 6000-100 for head and body phantoms respectively for ten hospitals in Abuja. The electrometer and ion chamber techniques were applied on ten (10) various CT scanners and were used to estimate the computed tomography dose index (CTDIw) and the results compared to the computed tomography dose index (CTDI) values for accuracy and validation purposes. The results showed the body phantom doses ranged from 0.31±0.01 mGy to 1.58± 0.002 mGy, while the head phantom doses ranged from 1.30±0.001 mGy to 1.94± 0.3 mGy. The mean dose ratios for head and body phantom were 1.67± 0.15Gy and 1.23±0.03Gy, respectively. The results indicate that the body phantom doses were within the acceptable limits of 1Gray, whereas the head phantom doses exceeded the recommended limits. The differences in CT doses between CT machines suggest a need for optimization of CT examinations protocol and QC measures in some CT establishments in Abuja hospitals.
Keywords: Computed Tomography, Phantoms, Radiation Dosage, Quality Control, Dosimetry

Introduction

Computed tomography is an imaging procedure that uses special X-ray equipment to produce cross-sectional images of the body within a short period of time. It is an important diagnostic tool because of its unique ability to offer clear images of bone, muscle, blood vessels, and different types of tissue where other imaging techniques are limited in the quality of images they can provide [1]. It can also be used to plan certain surgeries, guided biopsies, measure bone mineral density, detect injuries to internal organs, and has proven to be a valuable tool for the diagnosis and treatment of many musculoskeletal disorders. Computed tomography imaging is even used for the diagnosis and treatment of certain vascular diseases. Probably the most important aspect of computed tomography however, is its role in cancer treatment. It allows physicians to accurately detect and locate different types of cancers and plays an important part in radiation treatment planning process. Computed tomography is also used in creating a hybrid technology to maximize patient imaging techniques. The importance of computed tomography technology is without a doubt a vital aspect for the diagnosis and treatment of patients, and as advancements in computed tomography develop; patient care will continue improving [2].

However, CT has been therefore considered as a potential source of increased cancer risk as compared to other imaging modalities [3]. For instance, one head CT examination is equivalent to radiation dose of 100-150 conventional chest radiographs [4-5]. Also, one chest CT examination delivers about 400 times the dose delivered by a conventional chest X-ray examination [6-7]. CT is also known to constitute 30-40% of patient radiation dose which could cause damage on differentiating tissues (thyroid, gonads, breast, bone marrow etc) [8-9].

Based on this perspective, it is of interest to quantify the amount of radiation dose imparted to patients undergoing a CT examination, with the use of standard CT dosimetry Polymethyl Methacrylate (PMMA) cylindrical acrylic head and body phantoms techniques. This work has therefore provided an opportunity to determine and evaluate the radiation dose to patient and Quality Control (QC) parameters towards producing an optimized working

protocol for CT examinations. The results have also provided information on the status of radiation protection of the facilities at various centres of study in Abuja hospitals, and has also added significant information to the body of knowledge on the subject matter for the scientific community, hence the study.

Materials and Methods

Standard CT dosimetry polymethy methacrylate cylindrical acrylic (PMMA) head and body phantoms (PTW 30009, Freiburg, Germany). The PMMA CT phantom is a transparent plastic, which is lightweight for easy mobility and has a density of 1.19 ± 0.01 g/cm^3 with a thickness of 3 mm and each is a right circular cylinder [13]. The head and body phantoms have diameters of 16cm and 32cm, respectively, with lengths of 14-16 cm (available from several dosimeter and radiological accessory manufacturers). All phantoms have holes at a depth of 1 cm (center to phantom edge) from the outer surface, at the 90^0, 180^0, 270^0 and 0^0 normal clock positions referred to as the peripheral sites and along the cylinder axis as shown in the figure 1 below:

Figure 1: image of CT head phantom (small) and body phantom (large) [1]

The CT dose phantoms that are used in this study are the models 76-414 (head), 76- 415 (body) phantoms respectively. Each part contains five probe holes, one in the center and four around the perimeter, 90° apart and 1 cm from the edge. Each part includes five acrylic rods for plugging all the holes in the phantom. The CT dose phantoms are designed in accordance with standard for diagnostic X-ray systems [10]. Table 1 shows the CT phantoms specifications.

Table 1: Specifications of the CT phantoms [11-15]

Weight	Body phantom: 14.5 kg Head phantom: 3.6 kg
Optional accessories	Carrying Case (Model 89-414) CT Head Dose Phantom with five plugs (Model 76-414) CT Body Dose Phantom with five plugs (Model 76-415)

100-mm pencil Ion Chamber with integrated electrometer

The standard "pencil" ionization chamber, first described by [16] and [17] employ the principle of volume averaging [18]. The pencil ionization chambers are available with a diameter of 10 mm, a sensitive length of 100 mm, and an active volume of 3 cm^3, as shown in Figure 2.

Figure 2: image of CT ion chamber [1]

The CT chamber is designed for non-uniform exposure from a single scan or a number of scans [19]. Their response is designed to be uniform along the entire length of the sensitive volume, with a conversion factor determined in the conventional manner. The ionization chamber that is used in this study is the VICTOREEN CT Probe, model 6000-100 designed to be used for standard CT dosimetry PMMA cylindrical acrylic head and body phantoms. Its specifications are listed in Table 2. The chamber is connected, through 0.9 m of low noise flexible cable terminated with a male BNC size triaxial connector. It is designed to be readout on the NERO™ or Model 400M+ [18-19].

Table 2: Specifications of VICTOREEN CT Probe, model 6000-100 CT Probe **[18-19]**

Detector type	Vented air ionization chamber
Volume	3.2cm^3
Sensitive length	10.0 cm
Chamber	Material: Clear Acrylic Inside Diameter: 6.4 mm Wall Thickness: 54mg/cm^2
Electrode	Material: Aluminum. Diameter: 0.64 mm
Sensitivity	10 R cm/Nc
Factor Calibration	100 kVCP, 5.5 mm Al HVL
Energy Response	+5%, 1 mm Al to 10 mm Al HVL Uniformity along z axis: +3% over central 90% of active length
Beam Orientation	Normal to chamber axis
Phantom Adapter	Outside diameter: 1.27 ±0.04 cm

The electrometer that is used is a PTW DIA DOS E. It is a self contained, noninvasive X-ray test device. In a single exposure, it can measure simultaneously: kVp, exposure rate or air kerma rate and time. It is calibrated for both tungsten anode (W/Al) and Molybdenum (Mo/Mo) anode X- ray tubes. Additionally, it has an external ion chamber port that accepts a variety of accessory ionization chambers for various applications, including pencil shaped ionization chambers for CT dosimetry. It can compute the tube potential with ±3% accuracy. Five separate, selectable filter pairs ensure optimum accuracy over the maximum range with minimum filtration dependence. A separate internal ionization chamber measures tube output [19-20] as shown in Figure 3.

Figure 3: image of and electrometer [1]

Table 3: Measured quantities of Kilovoltage, Time and Exposure

Kilovoltage	Measured during the first 300 ms of exposure • kVp average • kVp effective • kVp maximum Accuracy: ±3%
Time	Measured during entire exposure; reference to 75% rise/fall kV time. Accuracy: Within 2% or 2 ms, whichever is greater Range: 1ms to 10 sec
Exposure	Measured during entire exposure, kVp corrected. Accuracy: ±10% Range: 10 mR to 10 R

For the measurement of the CT Dose Index, the chamber is positioned parallel to the rotation axis of the scanner inside a cylindrical phantom. For a single scan (except for a multislice), the primary beam does not usually cover more than about 10% of the full length of the chamber. At the same time, the CT chamber detects the scattered radiation generated in the phantom by the primary beam, thereby allowing quantification of the total exposure of a patient. This unique use of the CT chamber requires that the response of the active volume be uniform along its entire axial length, a restriction that is not required of other cylindrical full immersion chambers [18].

They are usually calibrated in terms of air kerma by exposing the entire sensitive volume to a uniform X-ray field because the dose profile rapidly falls to zero away from the position of the CT slice, the pencil ionization chamber also measures CTDI to a very good approximation [20].

For measurement, the chamber is mounted in such a way that its length axis corresponds to the axis of rotation of the gantry and that its centre corresponds to the centre of the slice, or the centre of the slices for a multi-slice scanner, Figure 3.3 shows the measurement with the ionization chamber made for a single rotation.

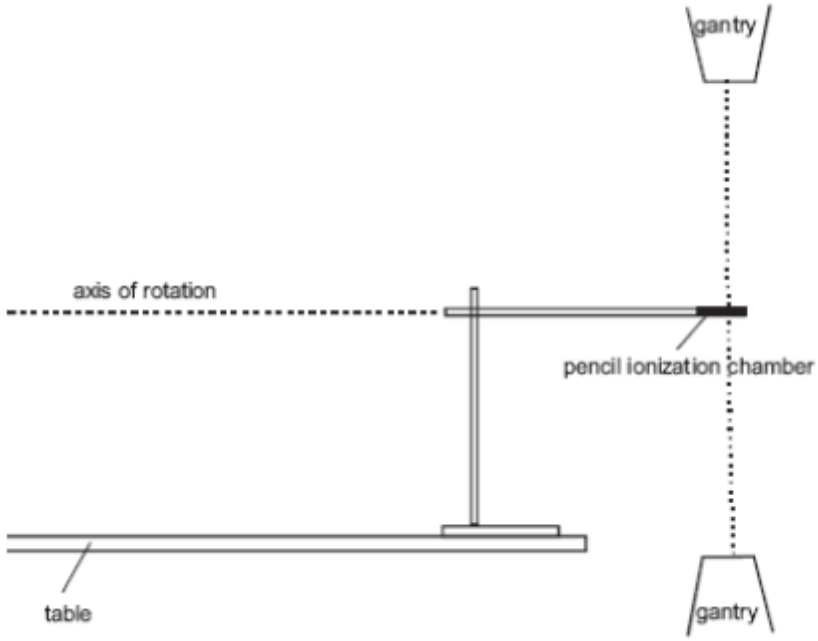

Figure 4: Schematic diagram of the arrangement for measurement of CTDI

Barometer (Pressure indicator D PI 800)

This a hand- held, light weight pressure test and measurement instrument ideally suited for use in the field for performing work such as calibration and repair, installation, maintenance, as well as in various manufacturing environments. The DPI 800 pressure indicator is available with a maximum of two internal pressure sensors. It has the following specifications: measuring ranges from 25 mbar to 700 bars, one or two internal sensors, transmitter calibration and switch test function as shown in Figure 5 [21].

Figure 5: Barometer (Pressure indicator D PI 800) (Digital, China)

Thermometer is a device that measures temperature or temperature gradient. It has two important elements

namely; (1) Temperature sensor (example the bulb of a mercury in- glass thermometer or the pyrometric sensor in an infra red thermometer) in which some change occurs with a change in temperature; and (2) some means of converting this change into a numerical value (example the visible scale that is marked on a mercury-in- glass thermometer or digital readout on an infrared model). Thermometers are widely used in technology and industry to monitor processes, in meteorology, medicine and in scientific research. The most recent official temperature scale of 1990 extends from 0.65K (-272.5^{0}C; -458.5^{0}F) to approximately 1,358K (1,085^{0}C; 1985^{0}F) as shown in Figure 6 [21].

Figure 6: Thermometer (Digital, China)

The computed tomography machines used for this work in ten centres were situated in Abuja, FCT. Measurements of Computed tomography dose index (CTDI) were carried out by a pencil shaped ionization chamber of active length 100 mm inserting in standard computed tomography (CT) Polymethyl methacrylate (PMMA) materials with PTW chamber type 30009, Freiburg, Germany dosimetry phantoms that is used frequently in CT dose measurement compose of a 32cm-diameter phantom to represent an adult chest, and a 16cm-diameter version to represent an adult head. Both are 15 cm thick (in the z-axis direction) and contain 1 cm diameter holes for insertion of the CT ion chamber probe. The holes on the phantoms are at the centre and at 1 cm depth at the 90^0, 180^0, 270^0 and 0^0 normal clock positions referred to as the peripheral sites.

The body phantom was first set up on the CT couch and centered at the isocenter of the scanner with the long axis of the phantom aligned with the z-axis of the scanner. The PTW pencil ion chamber which is connected to an electrometer with a cable was placed in the central hole of the phantom. Two horizontal lasers in the CT room were adjusted to be visible on the mid-line of the ion chamber and a vertical laser was also set to be visible at the middle of the phantom. This was done to properly align the phantom and the chamber on the couch. A piece of tape was put along the probe, attaching it on to the phantom to ensure that the probe is not dislodged within the phantom during scanning. A topogram image of the phantom was taken and used to select the volume to be scanned. The CTDI quality assurance measurements were activated for the first scan with the standard protocol of body examination for three readings at each point (one in centre and four points on peripheral of a phantom) at 90^0, 180^0, 270^0 and 0^0 normal clock positions represented as P1, P2, P3, P4 and C and subsequently the head phantom respectively as shown in (Tables 1 and 2). Charges were measured and recorded in each scan. The charges measured and recorded from the electrometer in charge mode, corrected for temperature and pressure were used to estimate $CTDI_w$ and DLP values and compare with CTDI and DLP console display on the CT in the study with the use of mathematical equations:

$$k_{TP} = \frac{(273.2+T)P_0}{(273.2+T_0)P} \quad (1)$$

$$C_{PMMA,100,c} = \frac{10}{NT} M_c N_{PKL,Q_o} k_Q k_{TP} \quad (2)$$

$$C_{PMMA,100,P} = \frac{10}{NT} M_P N_{PKL,Q_o} k_Q k_{TP} \quad (3)$$

$$CTDI_w = \frac{1}{3}(C_{PMMA,100,c} + 2C_{PMMA,100,P}) \quad (4)$$

$$DLP = CTDI_{vol} \times Scan\ length \quad (5)$$

The above equations, T is nominal slice thickness; N is number of tomographic slices simultaneously exposed (so that the nominal width of the irradiating beam is NT), k_{TP} is the correction factor for temperature and pressure, T is temperature measured in the study room, P is the pressure in the room, T_0 is temperature at reference condition, P_0 is air pressure at reference condition, N_{PKL}, Q_o is the dosimeter calibration coefficient in terms of the air kerma length product, k_Q is the factor which corrects for differences in the response of the dosimeter at the calibration quality and at the measurement quality Q of the clinical X-ray beam, M_c and M_p is the mean dose readings from the central chamber bore of the standard phantom and the mean dosimeter readings in the peripheral chamber bores, $C_{PMMA,\ 100,\ C}$ and $C_{PMMA,\ 100,\ P}$ is Polymethyl methacrylate (PMMA) computed tomography dose index at the centre and periphery of the chamber bores

Results

The study carried out and calculations leading to CT dose index, temperature and pressure corrections at Abuja hospitals are presented in Tables1 and 2 respectively.

Table 1: Dosimetry phantom readings for head at some hospitals in Abuja

Hospitals	CTDI(mGy)	$CTDI_w$(mGy)	Dose
1	19.18±0.004	10.38±0.004	1.85±0.004
2	49.8±0.03	35.88±0.03	1.39±0.03
3	38.50±0.02	25.18±0.02	1.53±0.02
4	36.60±0.02	23.78±0.02	1.54±0.02
5	70.0±0.90	37.32±0.90	1.88±0.90
6	30.18±0.001	23.30±0.001	1.30±0.001
7	39.81±0.1	25.12±0.1	1.58±0.1
8	38.52±0.1	20.61±0.1	1.87±0.1
9	67.46±0.3	34.84±0.3	1.94±0.3
10	20.8±0.001	11.19±0.001	1.86±0.001
		Mean Dose =	1.67±0.15 Gy

Table 2: Dosimetry phantom readings for body at some hospitals in Abuja

Hospitals	CTDI(mGy)	$CTDI_w$ (mGy)	Dose
1	10.05±0.01	7.18±0.01	1.39±0.01
2	10.8±0.004	7.9±0.004	1.37±0.004
3	9.57±0.01	18.59±0.01	0.51±0.01
4	7.30±0.01	4.68±0.01	1.56±0.01
5	6.3±0.01	20.02±0.01	0.31±0.01
6	8.93±0.002	5.66±0.002	1.58±0.002
7	7.95±0.01	5.08±0.01	1.56±0.01
8	5.04±0.0007	3.29±0.0007	1.53±0.0007
9	12.74±0.32	10.29±0.32	1.24±0.32
10	12.85±0.002	9.92±0.002	1.29±0.002
		Mean Dose =	1.23±0.03 Gy

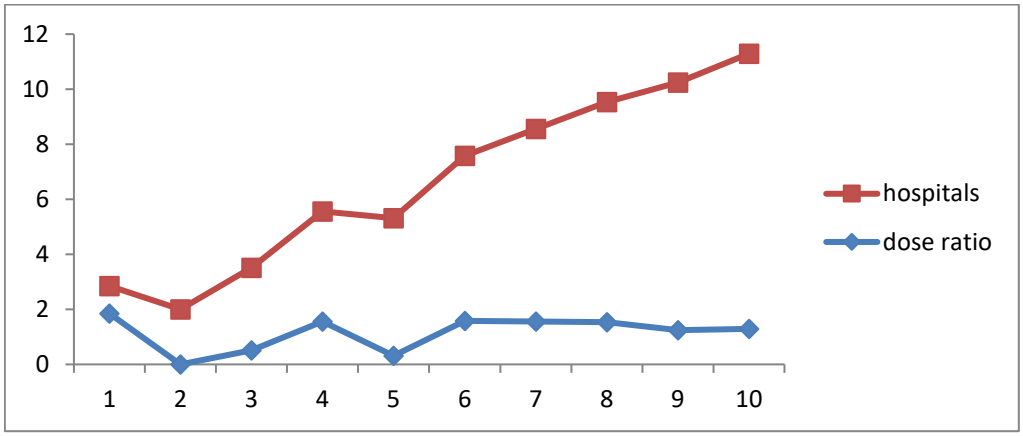

Figure 7: Hospitals to dose ratio for head phantoms

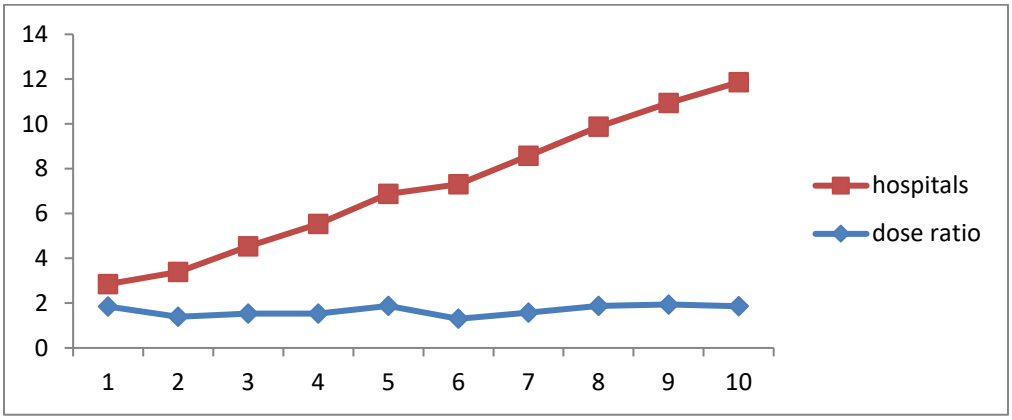

Figure 8: Hospitals to dose ratio for body phantoms

Discussion

Comparison of the results shows that doses for the same examinations varied from hospital to hospital as shown in Tables 1 and 2. The radiation doses for small phantoms with the same kVp and mA values are greater than those for large-sized phantoms [22-23], which mean that doses to the organs in the head are twice as high as those to the organs in the body using the same technique as shown in Tables 1 and 2. Other inconsistencies in the results obtained in this work such as variation in measured doses for the same values of kVp and mAs, increase in kVp and mAs not yielding a corresponding increase in dose sometimes may be as a result of the workload of the machine - as the electrons released hits the focus on the anode, a lot of heat is experienced at the point which increases the scattered radiation and reduces the transmitted rays, which in turn decreases the efficiency [3].

However, the study was found to be consistent with the reported values for CTDI of 49.6 mGy [24-28]. Most of the results met the American College of Radiology (ACR) CT accreditation requirement that the CTDI should be within the range of 40-60 mGy for the adult head protocol [29]. Similarly, the estimated CTDI measurement from standard body phantom values reported by 27.8 mGy [24 -25] and 12 mGy [28]. The results meet the American College of Radiology CT accreditation requirement that the CTDI should be within the range of 10-40 mGy for the adult body protocol [29].

The mean dose of the head is high than normal 1.0 Gray (Table 1). This is probably may be due to discrepancy of different types of protocols, user selection parameters (such as kVp, mAs, pitch and slice thickness) and differences in the design of computed tomography devices by the manufacturers [30].

Conclusion

This study provides valuable insights into CT dose quantities in ten radiological units of Abuja hospitals, establishing methods for assessing patient doses using phantoms and measuring computed tomography doses from CTDI ratios and machine console displays. Results indicate that body phantom doses were within acceptable limits, while head phantom doses exceeded recommended levels, highlighting the need for dose optimization. These findings emphasize the importance of quality control, proper calibration of CT machines, and protocol adjustments to minimize radiation exposure. Collaboration between radiological units and hospitals is essential to ensure patient safety, optimize CT protocols, and improve healthcare outcomes.

References

[1] Iortile, J.T and Ige T. A. (2022). **Measurement of Computed Tomography Dose Quantities at Some Radiological Units of Abuja Hospitals**. *African Journal of Medical Physics*; 4(1): 48-54.

[2] Abe, K. Hosono, M. Igarashi, T. Iimori, T. Ishiguro, M. Ito, T. Nagahata, T. Tsushima, H. Watanabe, H. (2020). **The 2020 national diagnostic reference levels for nuclear medicine in Japan**. *Ann Nucl Med* 34: 799–806.

[3] Albahiti, S.K. Barnawi, R.A. Alsafi, K. Khafaji, M. Aljondi, R,.Alghamdi, S.S. Awan, Z. Sulieman, A. Jafer, M. Tamam, N. Tajaldeen, A. Mattar, E.H. Al-Malki, K.M. Bradley, D. (2022). **Establishment of institutional diagnostic reference levels for 6 adult computed tomography examinations: results from preliminary data collection**. *Radiat. Phys. Chem*. 201: 110477.

[4] Alkadhi, H. Val, M. Runge, (2023). **The Future Arrived.** *Investigative Radiology*, Volume (58), 439-440.

[5] Stein, T. Rau, A. Russe, M. F. Arnold, P. Faby, S. Ulzheimer, S. Weis, M. (2023). **Photon-Counting**

Computed Tomography – Basic Principles, *Potenzial Benefits, and Initial Clinical Experience*. Volume (195), 691-698

[6] Dieckmeyer, M. Sollmann, N. Kupfer, K. Löffler, M.T. Paprottka, K.J. Jan S. Kirschke, J.S. Baum, T. (2023). **Computed Tomography of the Head.** *Clinical Neuroradiology,* Volume (33), 591-610.

[7] Si-Mohamed, S. Boccalini, S. Villien, M. Yagil, Y. Erhard, K. Boussel, L. Douek, P. (2023). **First Experience with a whole-body spectral photon-counting CT clinical prototype**. *Investigative Radiology*.

[8] Jason, K. E. Max W. Emre, N. Xinxin, W. Gregor, L. Girish, D. Mohammed, B. (2023). **Training Spiking Neural Networks Using Lessons from Deep Learning**. Volume (111), 1016-1054.

[9] Mkimel, M. Mesradi, M.R. El Baydaou,i R. Toufique, Y. Aitelcadi, Z. El Kharrim, A. and Hilali, A.(2019). **Assessment of Computed Tomography Dose Index (CTDI) using the Platform GEANT4/GATE**. *Elsevier*. Available online at *www.sciencedirect.com* accessed 10th February, 2024.

[10] Moawad, A.W. Fuentes, D.T. and ElBanan, M.G. (2022). **Artificial Intelligence in Diagnostic Radiology: Where Do We Stand, Challenges and Opportunities**. *Journal of Computer Assisted Tomography* 46(1): 78-90.

[11] Suh, Y. Joo, L. Sak, H. and Geu, R. (2022). **Feasibility of Aortic Annular measurements using non-contrast-enhanced cardiac Computed Tomography in preprocedural evaluation of Transcatheter Aortic valve replacement: A comparison with contrast enhanced Computed Tomography**. *Journal of Computer Assisted Tomography* 46(1): 50-55

[12] Abdulkadir, M.K. Piersson, A.D. Musa, G.M. Audu, S.A. Abubakar, A. Muftaudeen, B. Umana, J.E. (2021). **Assessment of diagnostic reference levels awareness and knowledge amongst CT radiographers**. *Egypt. J. Radiol. Nucl. Med*. 52 (1).

[13] Smith-Bindman, R. Wang, Y. Chu, P. (2019). **International variation in radiation dose for computed tomography examinations: Prospective cohort study**. *BMJ*. 364:1–12 35.

[14] AlNaemi, H. Tsapaki, V. Omar, A.J. AlKuwari, M. AlObadli, A. Alkhazzam, S. Aly, A. Kharita, M. H. (2020). **Towards establishment of diagnostic reference levels based on clinical indication in the state of Qatar**. *Eur. J. Radiol.* Open 7: 100282.

[15] Benamar, M. Housni, A. Sadiki, S. Amazian, K. Essahlaoui, A. Labzour, A. (2023). **Patient dose assessment in computed tomography in a Moroccan imaging department**. *Radioprotection* 58: 49–53.

[16] Buhari, M. Buhari, S. (2021). **Review on diagnostic reference levels (DRLs) for adult patients undergoing chest and abdomen computed tomography scan in Northern Nigeria**. *Afr. J. Environ. Nat. Sci. Res.* 4: 83–90.

[17] Dambele, M.Y. Bello, S.G. Ahmad, U.F. Jessop, M. Isa, N.F. Agwu, K.K. (2021). **Establishing a local diagnostic reference level for bone scintigraphy in a Nigerian Tertiary Hospital**. *J. Nucl. Med. Technol*. 49: 339–343.

[18] Damilakis, J. Vassileva, J. (2021). T**he growing potential of diagnostic reference levels as a dynamic tool for dose optimization.** *Phys. Med*. 84: 285–287.

[19] Shim, S. Saltybaeva, N. Berger, N. Macron, M. Alkadhi, H. and Boss, A. (2020). **Lesion detectability and radiation dose in spiral breast CT with photon-counting detector technology: a phantom study**. *Investigative radiology,* 55(8): 515-523

[20] Matthias, W. Matthias, D. Sabine, O. Michael, U. and Evelyn, N. (2022). **Spiral breast computed tomography with a photon – counting detector (SBCT): The future of breast imaging**. *European Journal of Radiology*, volume 157.

[21] Hakme, M. Rizk, C. Francis, Z. Fares, G. (2023). **Proposed national diagnostic reference levels for computed tomography examinations based on clinical indication, patient gender and size and the use of contrast in Lebanon**. *Radioprotection* 58: 113–121.

[22] Alabousi, M. Wadera, A. Kashif, A.M. (2021). **Performance of Digital Breast Tomosynthesis, Synthetic Mammography, and Digital Mammography in Breast Cancer Screening: A Systematic Review and Meta- Analysis**. *J Natl Cancer Inst*. 113(6): 680-690.

[23] Kuhl, C.K. 2023. **What the Future Holds for the Screening, Diagnosis, and Treatment of Breast Cancer**. *Radiology;* 306:e223338.

[24] Kang, T. Zhang, Z. Zhang, Y. Chen, E. Niu, Y. (2021). **A multi-provincial survey and analysis**

of radiation doses from pediatric CT in China. *Radiat. Med. Protect.* 2: 23–27.

[25] Lee, K. L. Beveridge, T. Sanagou, M. Thomas P. (2020). **Updated Australian diagnostic reference levels for adult CT**. *J. Med. Radiat. Sci.* 67: 5–15.

[26] Muhammad, N.A. Karim, M.K.A. Harun, H.H. Rahman, M.A.A. Azlan, R.N.R.M. Sumardi, N.F. (2022). **The impact of tube current and iterative reconstruction algorithm on dose and image quality of infant CT head examination.** *Radiat. Phys. Chem.* 200: 110272.

[27] Hussein, H. Abbas, E. Keshavarzi, S. Fazelzad, R. Bukhanov, K. Kulkarni, S. Au, F. Ghai, S. Alabousi, A. Freitas, V. (2023). **Supplemental Breast Cancer Screening in Women with Dense Breasts and Negative Mammography: A Systematic Review and Meta-Analysis.** *Radiology*; 306: e221785

[28] Oztek, M. A., Mossa-Basha, M., DeConde, R., Mogensen, M. A., Cross, N. M., Cohen, W., & Yuh, W. T. (2022). **Is a Close Follow-Up Computed Tomography Necessary for Acute Falcine and Tentorial Subdural Hematoma?** *Journal of Computer Assisted Tomography*, *46*(1), 97-102.

[29] Siegel, M.J. Raptis, D. and Bhalla, S. (2022). **Comparison of 100-Kilovoltage Tin Filtration with Advanced Modeled Iterative Reconstruction Protocol to an Automated Kilovoltage selection with Filtered Back Projection Protocol on Radiation Dose and Image Quality in Pediatric Non-Contrast Enhanced Chest Computed Tomography.** *Journal of Computer Assisted Tomography* 46(1): 64-70.

[30] Suzuki, S. Samejima, W. and Harashima, S. (2022). **In vitro study of the precision and accuracy of measurement of the vascular inner diameter on Computed Tomography Angiography using Deep Learning image Reconstruction: Comparison with Filtered back projection and iterative reconstruction**. *Journal of Computer Assisted Tomography* 46(1): 17-22.

Cite this article

Iortile J.T., Alumuku L., and Shaanika A. (2025). Radiation Dose Optimization in Computed Tomography Examinations: A comparative Analysis of Body and Head phantoms in some Radiological Units of Abuja Hospitals. FUAM Journal of Pure and Applied Science, **5**(**2**):36-44